

Zeeman relaxation of magnetically trapped Eu atoms

Yury V. Suleimanov*

Physical and Theoretical Chemistry Laboratory, University of Oxford, South Parks Road, Oxford OX1 3QZ, United Kingdom

(Received 30 September 2009; published 3 February 2010)

We perform rigorous quantum mechanical calculations for collisions between magnetically trapped Eu atoms to elucidate the results of recent experimental studies. We show that the relaxation from the maximally stretched $m_s = 7/2$ level is entirely determined by the magnetic dipole-dipole interaction and analyze the role of the electronic spin-exchange interaction in transitions from the lower-energy Zeeman levels. The relaxation of the $m_s = 5/2$ state is shown to be very sensitive to the spin-exchange parameter that determines the splitting between the lowest electronic states of the Eu dimer. We suggest that cold collision experiments with trapped atoms can be used as a tool for obtaining accurate information on the electronic spin anisotropy in complex molecules such as Eu_2 .

DOI: [10.1103/PhysRevA.81.022701](https://doi.org/10.1103/PhysRevA.81.022701)

PACS number(s): 34.50.-s, 32.60.+i, 34.20.-b, 31.10.+z

I. INTRODUCTION

Atomic ensembles can generally be cooled to ultracold temperatures using a combination of buffer-gas cooling and magnetic trapping [1–13]. The efficacy of buffer-gas cooling is determined by the electrostatic interaction anisotropy between atoms in the buffer-gas cell [14]. The anisotropy must be low to minimize Zeeman relaxation of atoms in the low-field-seeking levels induced by collisions with buffer-gas atoms. A number of recent experimental and theoretical studies of atomic collisions at cold temperatures revealed important information not only on the prospects for buffer-gas cooling of different atoms, but also on the electrostatic interaction anisotropy, which is of interest in a much broader context. For example, measurements of Zeeman relaxation in collisions of transition-metal (Ti and Sc) [4] and lanthanide (Tm, Er, Nd, Tb, Pr, Ho, Dy) [5] atoms with He atoms demonstrated the suppression of the orbital angular momentum interaction anisotropy for submerged open electronic shells ($3d$ and $4f$) [15–17].

Considerable effort has been recently made to cool and trap atoms with large magnetic moments, particularly, heavy metal atoms with zero electronic orbital angular momentum. Large magnetic moments lead to significant trap depths increasing the magnetic trapping efficiency. The absence of the electronic orbital angular momentum ensures suppression of the anisotropic electrostatic interactions between atoms to lowest order. However, in a series of studies using $^{52}\text{Cr}(^7S)$ atoms, efficient dipolar relaxation was found to prevent evaporative cooling, and the mechanism of the dipolar relaxation was investigated in detail both experimentally and theoretically [6–9, 18, 19]. Cooling in an optical trap was suggested as a remedy, and an ensemble of ^{52}Cr atoms was successfully Bose-condensed in a magneto-optical trap [20, 21]. Magnetic trapping at cold temperatures was extended to other atoms with large magnetic moments, such as $\text{Mn}(^6S)$ [10], Mn-Cr mixture [11], and $\text{Mo}(^7S)$ [12]. The trap loss was observed and inelastic rates of the order of 10^{-12} – 10^{-13} cm^3/s were measured in these experiments, suggesting the dominant role of the magnetic dipole interaction. Careful analysis of the relaxation of Mn atoms in a magnetic trap, however, revealed

an important contribution of the spin-exchange transitions on the background of the relaxation induced by the magnetic dipole-dipole interaction [10].

$\text{Eu}(^8S^{\circ})$ is another example of an atom with a large magnetic moment. Owing to zero orbital and large spin electronic angular momenta, atomic Eu was used for the first realization of buffer gas loading into a magnetic trap [13]. The atoms in the maximally stretched $m_s = 7/2$ (m_s is projection of the electronic spin s of the Eu atom on a space-fixed quantization axis) Zeeman level were trapped in a magnetic trap with the trap depth of 0.52 T at a temperature of 250 mK. A very long trap lifetime of atoms was observed (> 100 s). The decay of the trapped ensemble cooled to 170 mK was found to be mediated by two-body collisions with the effective loss rate $(2.5 \pm 1.5) \times 10^{-13}$ cm^3/s tentatively assigned to dipolar relaxation [13, 22]. Subsequent analysis [23] revealed that, in contrast to other S atoms, the lower-energy Zeeman levels of Eu, namely, $m_s = 5/2$ and $3/2$, are also amenable to trapping under the same conditions. However, the corresponding collisional loss rates were not measured.

In this paper, we analyze these studies of Eu and report the results of rigorous quantum scattering calculations of inelastic Eu-Eu collisions in a magnetic field. First, we examine the relaxation of atoms in the maximally stretched $m_s = 7/2$ level. We show that the dipolar relaxation provides the dominant mechanism of trap loss, while the effects of the hyperfine and spin-exchange interactions are negligible. Second, we analyze the role of the electronic spin-exchange interactions in determining transitions from the lower Zeeman states. The efficiency of Zeeman relaxation is shown to be strongly affected by the spin anisotropy suggesting that the measurements of trap loss rates for multiple Zeeman states may provide a sensitive probe of spin-exchange interactions in the Eu dimer.

The remainder of this paper is organized as follows. The computation details are described in Sec. II, Sec. III presents the results, and the conclusions are summarized in Sec. IV.

II. COMPUTATIONAL DETAILS**A. Dynamical calculations**

The methodology of the present calculations is based on the theory described in Refs. [14, 24–28]. The total Hamiltonian

*yury.suleimanov@chem.ox.ac.uk

of two Eu atoms in the presence of an external magnetic field can be written in atomic units as

$$\hat{H} = -\frac{1}{2\mu R} \frac{\partial^2}{\partial R^2} R + \frac{l^2}{2\mu R^2} + \hat{V}_{\text{es}} + \hat{V}_{\text{dip}} + \hat{H}_{\text{as}}, \quad (1)$$

where μ is the reduced mass of the Eu_2 molecule, R is the interatomic separation, and l is the orbital angular momentum of the collision complex. The \hat{V}_{es} operator in Eq. (1) corresponds to the electrostatic nonrelativistic interaction. The electronic interaction anisotropy between two S atoms with the nonzero electronic spins reduces to the splitting between molecular states with different total electronic spin S , which can be referred to as the *spin anisotropy* [14]. In this case, \hat{V}_{es} can be defined in terms of the Born-Oppenheimer interaction potentials $V_S(R)$ of the diatomic molecule as

$$\hat{V}_{\text{es}} = \sum_{S, M_S} |SM_S\rangle V_S(R) \langle SM_S|, \quad (2)$$

where M_S is the projection of S on a space-fixed quantization axis.

The operator \hat{V}_{dip} in Eq. (1) describes the magnetic dipole-dipole interaction, which in the space-fixed coordinate frame is given by [25]

$$\hat{V}_{\text{dip}} = -\sqrt{\frac{24\pi}{5}} \frac{\alpha_{\text{fs}}^2}{R^3} \sum_{q=0, \pm 1, \pm 2} (-1)^q Y_{2-q}[s_a \otimes s_b]_q^{(2)}, \quad (3)$$

where α_{fs} is the fine-structure constant [29], and s_a and s_b are the electronic spin angular momenta of the two Eu atoms (labeled as a and b).

The asymptotic Hamiltonian \hat{H}_{as} in Eq. (1) is the sum of the operator \hat{H}_z , which describes the interaction of Eu atoms with the magnetic field B , and the operator of atomic hyperfine interaction \hat{H}_{hf}

$$\hat{H}_{\text{as}} \equiv \hat{H}(R \rightarrow \infty) = \hat{H}_{\text{hf}} + \hat{H}_z. \quad (4)$$

If the quantization z axis is chosen in the direction of B , the Zeeman Hamiltonian \hat{H}_z takes the form

$$\hat{H}_z = \sum_{\alpha=a, b} \left[g_L \mu_B s_{\alpha z} - \frac{\mu_n^\alpha}{i_\alpha} i_{\alpha z} \right] B, \quad (5)$$

where g_L is the Landé g factor [1.99 for $\text{Eu}(^8S^\circ)$] [23], $s_{\alpha z}$ is the z component of the electronic spin momentum of the corresponding Eu atom, μ_n^α are the nuclear magnetic moments, and $i_{\alpha z}$ is the z component of the nuclear spin momentum i_α of the corresponding Eu atom.

The operator \hat{H}_{hf} for the Eu atoms has the form [23]

$$\hat{H}_{\text{hf}} = \sum_{\alpha=a, b} A_\alpha i_\alpha s_\alpha + B_\alpha \frac{\frac{3}{2} i_\alpha s_\alpha (2i_\alpha s_\alpha + 1) - i_\alpha^2 s_\alpha^2}{2i_\alpha (2i_\alpha - 1) s_\alpha (2s_\alpha - 1)}, \quad (6)$$

where A_α is the hyperfine magnetic dipole coupling constant and B_α is the hyperfine electric quadrupole coupling constant. Hyperfine constants for the naturally occurring Eu isotopes are given in Table I.

The total wave function of the Eu-Eu collision system is expanded as follows

$$\Psi = R^{-1} \sum_{\beta l m_l} F_{\beta l m_l}(R) \psi_\beta |l m_l\rangle. \quad (7)$$

TABLE I. Natural abundances of Eu isotopes, nuclear spins, and hyperfine constants. Constants taken from Ref. [30].

Isotope	Natural abundance (%)	Nuclear spin (i)	A (MHz)	B (MHz)
^{151}Eu	47.81	5/2	-20.05	-0.7
^{153}Eu	52.19	5/2	-8.85	-1.78

Here $F_{\beta l m_l}(R)$ is the expansion coefficient, $|l m_l\rangle$ is the eigenfunction of the l^2 operator, m_l is the projection of l on the magnetic field axis, and ψ_β is the eigenfunction of the asymptotic Hamiltonian

$$\hat{H}_{\text{as}} \psi_\beta = \epsilon_\beta \psi_\beta, \quad (8)$$

where ϵ_β is the asymptotic energy of the collision channel β .

Different angular momentum coupling schemes can be used to represent ψ_β , but none of them provides the eigenchannel representation for the asymptotic Hamiltonian \hat{H}_{as} in the presence of a magnetic field. For strong magnetic fields, the collision theory is best formulated in the fully uncoupled space-fixed representation of the wave function [26]

$$\psi_\beta^0 = |s_a m_{s_a}\rangle |i_a m_{i_a}\rangle |s_b m_{s_b}\rangle |i_b m_{i_b}\rangle, \quad (9)$$

where m_{s_α} and m_{i_α} are the projections of s_α and i_α on the magnetic field axis. The transformation from basis (9) to the asymptotic channel functions ψ_β can then be constructed numerically for each value of the magnetic field by diagonalizing the matrix of \hat{H}_{as} [25]. Our choice of the representation (9) is motivated by high magnetic fields used in the experiment to trap Eu atoms [13, 23]. Nonzero off-diagonal matrix elements of H_{as} in representation (9) are given by the atomic hyperfine interaction, which is significantly weaker in comparison with the Zeeman splitting at high fields. [According to Table I, the hyperfine constants A and B for Eu are on the order of MHz, while $1\mu_B = 14\text{ GHz/T}$. At magnetic fields $B > 0.005\text{ T}$, the diagonal elements of \hat{H}_{as} in the basis (9) are very close to the exact Zeeman eigenenergies.]

The Zeeman Hamiltonian \hat{H}_z given by Eq. (5) is diagonal in the uncoupled basis (9). The matrix elements of the \hat{V}_{es} operator can be obtained using the transformation between the total electronic spin $|SM_S\rangle$ representation and the uncoupled representation (9), as described in Ref. [14]. The electrostatic interaction mixes states with different m_{s_a} and m_{s_b} but induces no coupling between states with different $m_{s_a} + m_{s_b}$. The matrix elements of \hat{V}_{dip} given by Eq. (3) can be evaluated analytically by rewriting the components of the tensor $[s_a \otimes s_b]^{(2)}$ in terms of the ladder operators $s_{\alpha\pm}$ as suggested in Refs. [25, 26]. The resulting matrix elements couple states with different m_{s_a} , m_{s_b} , and m_l but the sum $m_{s_a} + m_{s_b} + m_l$ is conserved. The selection rules for the matrix elements of \hat{V}_{dip} are $l - l' = 0, 2$ and $l = l' \neq 0$, and $M_S - M'_S = 0, \pm 1, \pm 2$. The hyperfine interaction couples states with different m_{i_a} and m_{i_b} , but conserves the total spin angular momentum of the atom f_α and its projection on the magnetic field axis $m_{f_\alpha} = m_{s_\alpha} + m_{i_\alpha}$. The nonvanishing matrix elements of \hat{H}_{hf} correspond to transitions with $m_{s_\alpha} - m'_{s_\alpha} = 0, \pm 1, \pm 2$ and $m_{i_\alpha} - m'_{i_\alpha} = 0, \mp 1, \mp 2$.

There are two naturally occurring isotopes of Eu, namely, ^{151}Eu and ^{153}Eu . In principle, three types of collisions should be examined and the results should be averaged according to the natural abundances of the isotopes. In addition, one should also take into account symmetry considerations for collisions between indistinguishable particles (see, e.g., Refs. [31,32]). However, both isotopes have almost equal natural abundances, the same nuclear spin, and similar hyperfine constants (see Table I). As indicated in the following section, the difference between Eu isotopes is found to be negligible at the high magnetic fields which are considered in this work ($B \geq 0.05$ T). For most of our calculations, we therefore consider only collisions between different isotopes, $^{151}\text{Eu} + ^{153}\text{Eu}$.

The substitution of expansion (7) into the Schrödinger equation with Hamiltonian (1) results in a system of coupled differential equations for the expansion coefficients $F_{\beta l m_l}(R)$. The scattering S -matrix elements are obtained by applying appropriate boundary conditions to the solutions $F_{\beta l m_l}(R)$ in the asymptotic region [26]. The cross sections for elastic and inelastic energy transfer are computed from the S -matrix elements as shown in Ref. [26]. For collisions between two identical Eu isotopes, an additional symmetrization procedure is performed. (The details of the symmetrization in the case of indistinguishable particles can be found in Ref. [32].) The system of closed coupled equations is propagated using the log-derivative propagator of Manolopoulos [33] on a grid of R from 2.0 to 200 Å with an integration step of 0.05 Å. The propagation matrix is then transformed to the representation in which \hat{H}_{as} is diagonal, before the scattering S matrix is constructed. The scattering calculations for collisions between $^{151}\text{Eu}(m_s = 7/2)$ and $^{153}\text{Eu}(m_s = 7/2)$ were performed at different magnetic fields in the range from 0.05 to 0.52 T and 300 collision energies E_{coll} covering, with a variable step, the interval from 10^{-7} to 1 cm^{-1} . Up to 14 partial waves were included in the basis to ensure convergence of the cross sections in the entire range of the collision energies to within 10%. We also performed calculations for the lower initial Zeeman state $m_s = 5/2$ at selected values of E_{coll} and B for collision between different isotopes. For these calculations, eight partial waves in the basis were found to be sufficient to achieve convergence. Since \hat{V}_{dip} —the only operator that couples different partial waves—does not couple channels with l of different parity, we performed calculations for even and odd partial waves separately and summed the results to obtain the total cross sections. In addition, we found that states with $m_s \leq +1/2$, $m_s \leq -1/2$, and $m_s \leq -3/2$ do not affect the results and can be excluded from expansion (7) for, respectively, $^{151}\text{Eu}(m_s = 7/2) + ^{153}\text{Eu}(m_s = 7/2)$, $^{151}\text{Eu}(m_s = 7/2) + ^{153}\text{Eu}(m_s = 5/2)$, and $^{151}\text{Eu}(m_s = 5/2) + ^{153}\text{Eu}(m_s = 5/2)$ collisions. To first order, these channels are not coupled by any of the interactions entering Eq. (1) with the initial states $m_s = 7/2$ and $5/2$ considered in this work.

B. Interaction potentials

The interatomic interaction operator \hat{V}_{es} is determined by Eq. (2) through the set of the Born-Oppenheimer potentials

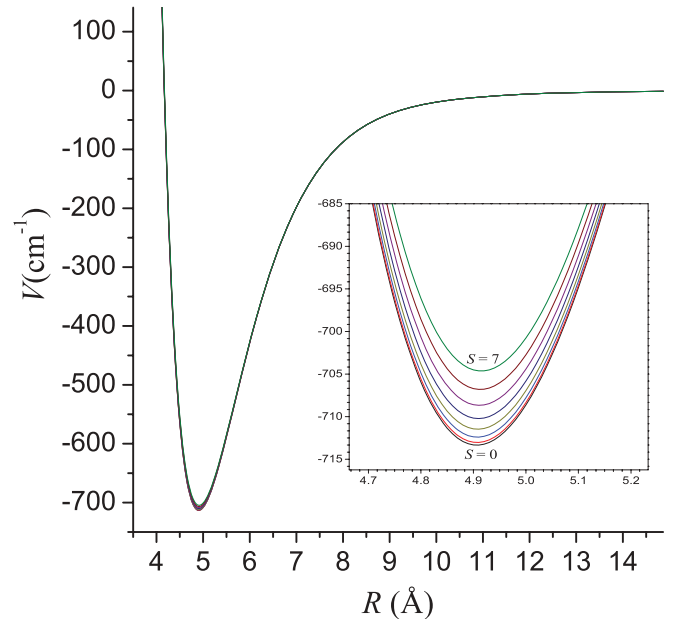


FIG. 1. (Color online) *Ab initio* electronic potentials arising from the $\text{Eu}(^8S^{\circ}) + \text{Eu}(^8S^{\circ})$ asymptote. Adapted from the data of Ref. [34]. Inset: behavior of the *ab initio* potentials in the region of the interaction minimum.

V_S . The total spin S of Eu_2 may take the values from 0 to 7 that correspond to eight electronic states $^1\Sigma_g^+$, $^3\Sigma_u^+$, $^5\Sigma_g^+$, $^7\Sigma_u^+$, $^9\Sigma_g^+$, $^{11}\Sigma_u^+$, $^{13}\Sigma_g^+$, and $^{15}\Sigma_u^+$ in the conventional LS -coupling notations. For the scattering calculations reported here, the *ab initio* based potential model from Ref. [34] was implemented. In brief, it utilizes the Heisenberg spin-exchange model [35,36] to express the potentials in the following form [34]:

$$V_S(R) = V_{S=7}(R) - \frac{1}{2}J(R)[S(S+1) - 56], \quad (10)$$

where $V_{S=7}(R)$ is the interaction potential for the spin-polarized electronic state $S = 7$ and $J(R)$ is the spin-exchange parameter. These two parameters were calculated using a combination of accurate single and multi reference *ab initio* methods in an extended basis set [34]. The computed interaction potentials for Eu_2 are shown in Fig. 1.

The *ab initio* calculations validated the proposed Heisenberg model and demonstrated very weak antiferromagnetic spin coupling [34]. The effective value of J is equal to -0.3 cm^{-1} , while the energy difference between the lowest $S = 0$ and highest $S = 7$ states at the equilibrium distance of 4.92 Å amounts to only 9 cm^{-1} (see Fig. 1). The coupling is so weak because the spin-bearing $4f^7$ atomic shells are screened by the outer closed $6s^2$ atomic shells, which keeps their atomic character in the dispersion-bound Eu_2 dimer. This effect can be considered as the suppression of spin exchange (or spin anisotropy) by analogy to similar effects of the suppression of orbital angular momentum anisotropy observed in lanthanide atoms with nonzero electronic orbital angular momenta [16,17,37]. However, such small splittings are comparable to the accuracy of quantum chemistry calculations [34] and no reliable experimental data are available for Eu_2 to

assess them. It is therefore of great interest to elucidate the sensitivity of cold collision dynamics to the magnitude of the spin-exchange energy.

III. RESULTS

In order to reproduce the experimental measurements and elucidate the mechanism of spin relaxation in Eu-Eu collisions, we performed detailed scattering calculations for Eu atoms initially in the maximally stretched $m_s = 7/2$ level. First, we considered three types of collisions between different Eu isotopes at $B = 0.05$ T and different values of E_{coll} in the interval from 10^{-7} to 1 cm^{-1} . The calculations for different hyperfine states ($m_{i_\alpha} = -5/2, \dots, +5/2$; $\alpha = a, b$) reveal strong suppression of the hyperfine effects in the relaxation process. The cross sections for Zeeman relaxation, as well as for elastic scattering, for all combinations of initial m_{i_a} and m_{i_b} states are the same to within 3%. Furthermore, the cross sections calculated for different types of collisions do not differ by more than a few percent (taking into account the presence of a symmetrization factor of 2 for collisions between identical isotopes with $m_{i_a} = m_{i_b}$). Such a small effect of the hyperfine interaction is consistent with the experimental observation of the persistence of all trapped hyperfine sublevels of the $m_s = 7/2$ manifold throughout the trap lifetime [22]. All hyperfine substates, including the doubly polarized state with $m_s = 7/2$ and $m_i = 5/2$, should therefore have almost the same speed of depopulation in the magnetic trap. The doubly polarized state is, however, immune to the hyperfine-induced inelastic collisions because there are no other states with the same values of f and m_f . This indicates that the hyperfine-unmodified, state-independent dipolar relaxation (i.e., when different hyperfine substates have equal dipolar relaxation rates) is predominant in the trap loss mechanism since other possible pathways of inelastic scattering, including spin exchange and hyperfine-modified dipolar relaxation, are mediated by the hyperfine interactions and should therefore be inefficient. To confirm this, we performed additional calculations with the terms \hat{V}_{dip} and \hat{H}_{hf} omitted from Eq. (1). The results of these calculations show that the Zeeman relaxation cross sections computed without \hat{V}_{dip} decrease by two to three orders of magnitude, whereas those computed without \hat{H}_{hf} decrease only by a few percent. We also verified that our code produces zero inelastic cross sections in a calculation without \hat{V}_{dip} for collisions between Eu atoms in the maximally stretched hyperfine state. The insignificant role of the hyperfine interaction at high magnetic fields, small difference in atomic masses, almost equal natural abundances, and the same nuclear spins of the Eu isotopes (see Table I), implies that, to a good approximation, we can consider only collisions between different isotopes. The remaining computations were therefore performed only for this case and only for one combination of the nuclear substates $m_{i_a} = m_{i_b} = 1/2$.

Figure 2 shows the energy dependence of the elastic cross section σ_{elastic} calculated for collision between $^{151}\text{Eu}(m_{s_a} = 7/2, m_{i_a} = 1/2)$ and $^{153}\text{Eu}(m_{s_b} = 7/2, m_{i_b} = 1/2)$ atoms at the magnetic field value $B = 0.1$ T. Calculations at other values of B established that the elastic scattering is largely insensitive

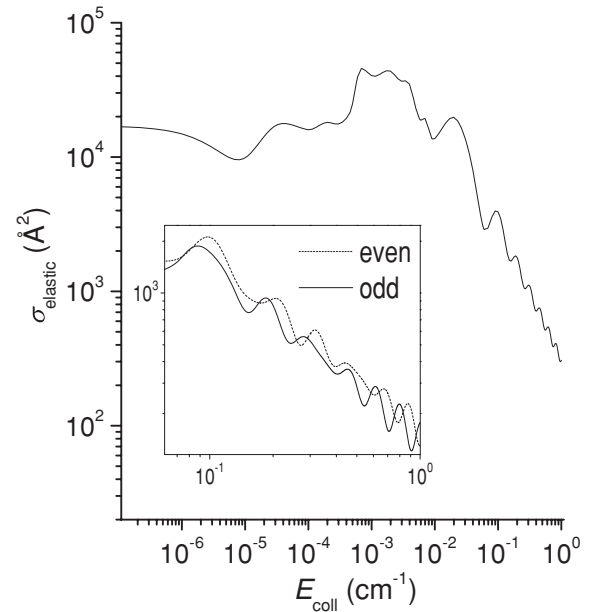


FIG. 2. Cross section for elastic energy transfer induced by collisions of ^{151}Eu with ^{153}Eu both initially in the hyperfine substate $m_i = 1/2$ of the $m_s = 7/2$ manifold as a function of the collision energy. Inset: components of the elastic scattering cross sections with odd and even l .

to the strength of the applied field. The elastic cross section displays several broad resonances in the interval between 10^{-1} and 1 cm^{-1} . The inset of Fig. 2 shows that the peaks of the cross sections calculated for even and odd partial waves in this interval are shifted, resulting in a broadening of the resonances after the summation over even and odd l . In the limit of vanishing collision energy, the elastic cross section tends to a constant value, in agreement with the Wigner law for s -wave scattering [38,39].

Figure 3 presents the inelastic cross sections $\sigma_{\text{inelastic}}$ calculated for the same initial states and the magnetic field values $B = 0.05, 0.1,$ and 0.5 T. The energy dependence of $\sigma_{\text{inelastic}}$ is similar at different values of B . The relaxation cross section rises rapidly as $1/\sqrt{E_{\text{coll}}}$ with decreasing energy in agreement with the Wigner threshold law [38,39]. In the energy interval between 10^{-4} and 10^{-2} cm^{-1} , the cross sections show a rich structure due to shape resonances. The positions of the resonances are independent of the magnetic field. A partial-wave analysis of the cross sections indicates that the odd and even values of l are responsible for resonances of different types. The inset of Fig. 3 demonstrates that the cross sections calculated for odd partial waves contribute to one broad resonance near 2×10^{-4} cm^{-1} and the dense manifold of resonance peaks above 1×10^{-3} cm^{-1} , whereas those calculated for even partial waves contribute only to two broad resonances near 7×10^{-4} and 4×10^{-3} cm^{-1} . We note that a similar combination of broad and narrow resonances was observed in the previous calculations for collisions of ^{52}Cr atoms initially in the $m_s = 3$ state [19]. The results in Fig. 3 also show that, at larger magnetic fields, $\sigma_{\text{inelastic}}$ decreases slightly because of the larger Zeeman splitting and the energy-gap law [27]. For high magnetic fields, the Zeeman splitting is so large that the centrifugal barrier in the final

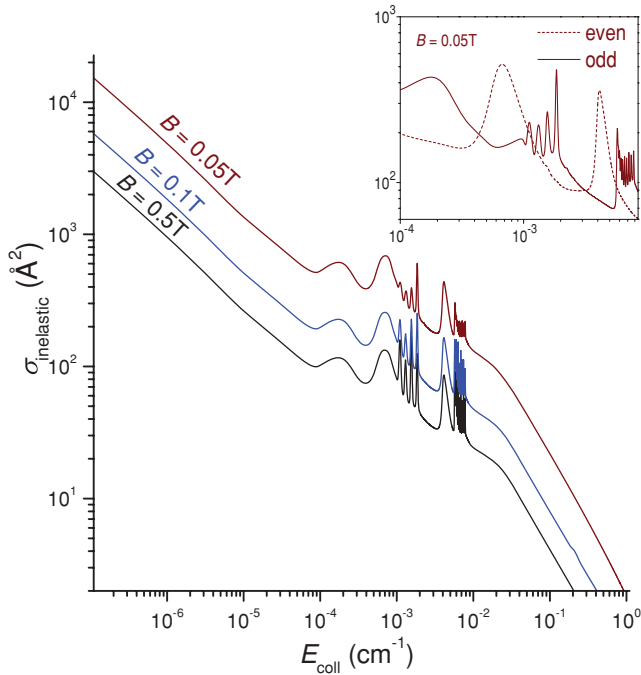


FIG. 3. (Color online) Cross sections for inelastic energy transfer induced by collisions of ^{151}Eu with ^{153}Eu both initially in the hyperfine substate $m_i = 1/2$ of the $m_s = 7/2$ manifold as functions of the collision energy. Inset: components of the inelastic scattering cross sections with $l = \text{even}$ and $l = \text{odd}$ at $B = 0.05$ T.

channel (which tends to suppress the transition probability with decreasing B) becomes negligible.

The rate constants for elastic energy transfer and Zeeman relaxation were obtained by Boltzmann averaging of the cross sections in Figs. 2 and 3. The calculated rate constants are shown in Fig. 4 as functions of the temperature in the range from 10^{-5} to 0.25 K at different values of B . Figure 4 shows that, as the temperature decreases, the field-independent elastic rate constant passes through a maximum near 10^{-2} K and decreases at lower temperatures. The inelastic rate constants also exhibit maxima near 10^{-2} K, which apparently originate from the broad shape resonances displayed in Fig. 3. The lower panel of Fig. 4 shows that the ratio of the rates for elastic scattering and spin relaxation γ decreases with decreasing temperature, especially below 10^{-3} K. This suggests that the loading temperatures of 170–250 mK achieved in a magnetic trap [13] can be somewhat lowered by evaporative cooling, but, for temperatures less than a few mK, this method should be quite inefficient. These conclusions are in qualitative agreement with the experimental and theoretical observations for ^{52}Cr [9,18,19].

We have also evaluated the inelastic rate constant $\Gamma_{\text{inelastic}}$ for the total Zeeman relaxation in a magnetic trap. In the experiment, most of the Eu atoms (>90%) were subjected to magnetic fields varying from 0.05 to 0.52 T and the density of the trapped atoms was assumed to have a Boltzmann distribution over B [13,23]. Under the assumption that the loss is due to collisions between atoms in the maximally stretched $m_s = 7/2$ level, the two-body trap loss rate constant was found to be $\Gamma_{\text{inelastic}} = (2.5 \pm 1.5) \times 10^{-13} \text{ cm}^3/\text{s}$ at 170 mK [13]. To account for the experimental conditions, we integrated

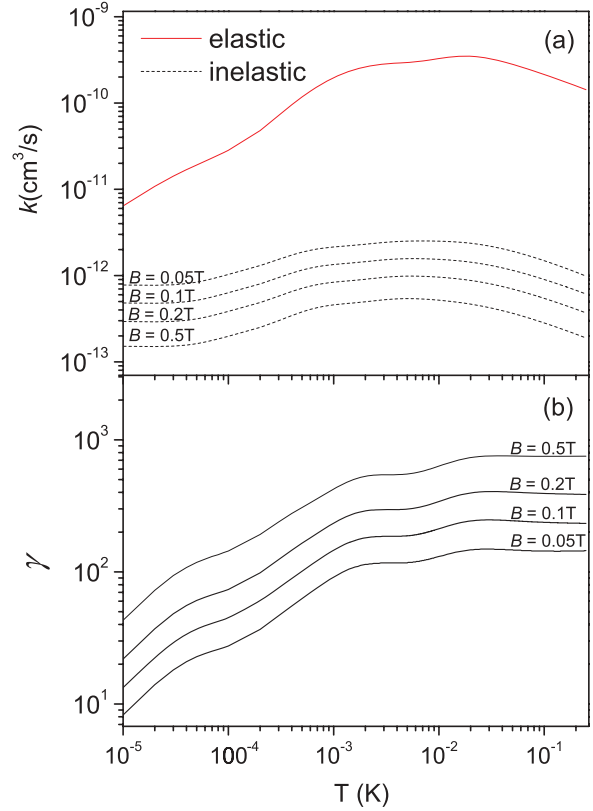


FIG. 4. (Color online) (a) Rate constants for collisions of ^{151}Eu and ^{153}Eu in the maximally stretched $m_s = 7/2$ state as functions of the temperature for field-independent elastic energy transfer (solid curve) and inelastic Zeeman relaxation (broken curves). (b) Ratio (γ) of rate constants for elastic scattering and Zeeman relaxation.

the field-dependent inelastic rate constants with a normalized Boltzmann distribution function in the range of the applied fields. These calculations yield $\Gamma_{\text{inelastic}} = 8.6 \times 10^{-13} \text{ cm}^3/\text{s}$, in reasonable agreement with the measured value.

As mentioned above, the *ab initio* calculations revealed significant suppression of the exchange interaction in the Eu_2 complex, which can be attributed to the effect of the submerged valence f -shell under a spherical closed s -shell in Eu atoms. To explore the sensitivity of the Zeeman relaxation from different Zeeman states to the spin anisotropy and elucidate the consequences of its suppression, we carried out a series of calculations with varying interaction potentials. As before, we considered collisions between different isotopes. The spin anisotropy of the interaction potential operator used in our computations is given by the Heisenberg exchange interaction in Eq. (10). The modified interaction potentials were constructed by replacing the computed exchange parameter $J(R)$ in Eq. (10) by a modified one, $\tilde{J}(R) = \eta J(R)$, with η varying in the interval from 0 (zero spin anisotropy) to 5 (maximum spin anisotropy considered here). According to Eq. (10), the $V_{S=7}$ potential remained unaffected by this modification, while the other potentials corresponding to $S = 0-6$ were subject to change. The splitting between the potentials $\Delta E_{0,7}$ calculated as the difference between $V_{S=7}$ and $V_{S=0}$ at $R = 4.92 \text{ \AA}$ —a distance close to equilibrium for all potentials—varied from 0 ($\eta = 0$) to 44 ($\eta = 5$) cm^{-1} . Using the modified potentials

we studied three types of collisions between different isotopes involving the highest $m_s = 7/2$ and lower-lying $m_s = 5/2$ Zeeman states, namely, $^{151}\text{Eu}(m_{s_a} = 7/2) + ^{153}\text{Eu}(m_{s_b} = 7/2)$, $^{151}\text{Eu}(m_{s_a} = 7/2) + ^{153}\text{Eu}(m_{s_b} = 5/2)$, and $^{151}\text{Eu}(m_{s_a} = 5/2) + ^{153}\text{Eu}(m_{s_b} = 5/2)$. As in our previous calculations, we considered the initial nuclear states with $m_{i_a} = m_{i_b} = 1/2$ but note that the Zeeman relaxation of lower magnetic states should be more sensitive to the hyperfine interaction in the presence of a stronger spin-exchange interaction. To explore the contribution of the magnetic dipolar relaxation, we also repeated the calculations with V_{dip} set to zero.

Figure 5 presents the dependences of the computed inelastic cross sections on $\Delta E_{0,7}$ at a magnetic field strength of 0.1 T and a collision energy of 0.001 cm^{-1} . We verified that the qualitative trends discussed below remain valid for all

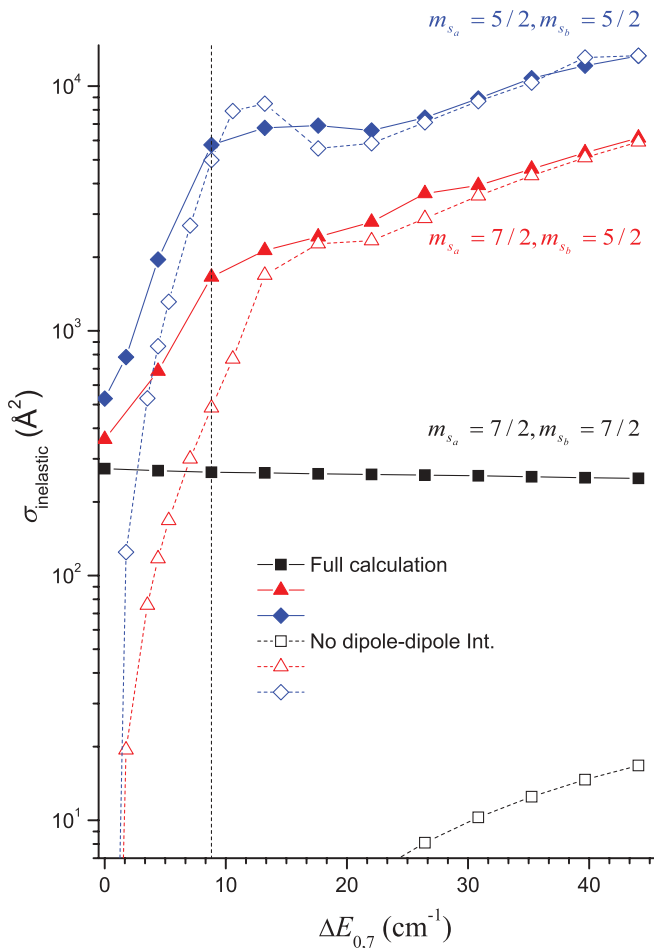


FIG. 5. (Color online) Cross sections for inelastic collisions between $^{151}\text{Eu}(m_{s_a})$ and $^{153}\text{Eu}(m_{s_b})$ as functions of the splitting $\Delta E_{0,7}$ between the interaction potentials of the Eu_2 molecule. Squares – $m_{s_a} = 7/2$ and $m_{s_b} = 7/2$; triangles – $m_{s_a} = 7/2$ and $m_{s_b} = 5/2$; diamonds – $m_{s_a} = 5/2$ and $m_{s_b} = 5/2$. Both Eu atoms are initially in the hyperfine substate $m_i = 1/2$. The collision energy is 0.001 cm^{-1} and the magnetic field is 0.1 T. The cross sections were obtained from the full calculation (solid lines and filled symbols) and calculation without the \hat{V}_{dip} term (dashed lines and open symbols). Vertical dashed line indicates the unmodified splitting corresponding to the original *ab initio* calculations.

combinations of initial hyperfine substates and the other values of B and E_{coll} considered in this work. The spin anisotropy conserves both S and M_S , and therefore it cannot play any role in collisions of atoms in the maximally stretched electronic spin state. Figure 5 confirms this. Calculations without V_{dip} indicate that transitions from lower Zeeman states can be driven by dipolar relaxation, but only when the spin anisotropy is suppressed. Figure 5 shows that, in the absence of splitting between the adiabatic potentials ($\eta = 0$), these collisions are entirely magnetic dipole induced, and the cross sections do not differ significantly from those obtained for $m_{s_a} = m_{s_b} = 7/2$. The role of the electronic spin-exchange interaction, however, increases quickly with the splitting between the potentials. The calculations with the splitting $\Delta E_{0,7} \approx 9 \text{ cm}^{-1}$ ($\eta = 1$) revealed different mechanisms of Zeeman relaxation of the $m_s = 5/2$ state depending on the initial state of the collision partner. The results denoted by the vertical dashed line in Fig. 5 show that the magnetic dipole interaction plays the dominant role when the collision partner is in the $m_s = 7/2$ state, but when both atoms are initially in the $m_s = 5/2$ state, the spin anisotropy plays the dominant role. The collision dynamics of subjacent Zeeman states ($m_s \leq 7/2$) in a magnetic trap is determined predominantly by collisions involving the maximally stretched state ($m_s = 7/2$). Therefore, the *ab initio* results establish the dipolar relaxation to be the main binary loss mechanism for the $m_s = 5/2$ state. At higher values of $\Delta E_{0,7}$ ($\eta > 1$), the contribution of the dipolar relaxation quickly becomes negligible, and this tendency is more prominent for $m_{s_a} = m_{s_b} = 5/2$.

The results presented in Fig. 5 show that the Zeeman relaxation of lower Zeeman states is very sensitive to spin anisotropy. The inelastic cross sections calculated for collisions involving the $m_s = 5/2$ state increase approximately by a factor of 20 as $\Delta E_{0,7}$ increases from 0 to 44 cm^{-1} making the Zeeman relaxation more efficient than that of the maximally stretched $m_s = 7/2$ state. Recent analysis of the experimental data [23] showed that the $m_s = 5/2$ and $m_s = 3/2$ states can be trapped under the same experimental conditions as for the $m_s = 7/2$ state and its hyperfine substates. These states persisted throughout the trap lifetime. Our results demonstrate that this may be due to the spin anisotropy suppression. Unfortunately, Zeeman relaxation rates for the co-trapped levels were not estimated in the experiment but, if measured, they could provide accurate information on the electronic spin-exchange interaction in the Eu dimer. Little is known in the literature about the electronic structure of the Eu_2 molecule (see Ref. [34]). It was probed in a series of experiments [40–43] which, however, provided very scarce and contradictory information. Previous theoretical works met with difficulties and even failed to establish with certainty the multiplicity of the ground electronic state of the dimer [44,45]. We have used accurate *ab initio* potentials recently computed for all spin states arising from the interaction of two $\text{Eu}(^8S^{\circ})$ atoms [34]. Our results show that cold collision experiments with multiple Zeeman states may provide tests of the *ab initio* results. We note that Eu atoms were detected in the trap by laser absorption spectroscopy with a resolution sufficient to distinguish transitions from $m_s = 7/2, 5/2$, and $3/2$ (see Fig. 5 in Ref. [23]) suggesting that such state-selective measurements of collision rates should be feasible.

IV. SUMMARY

The main results of our theoretical study of the dynamics of collisions between magnetically trapped Eu atoms can be summarized as follows.

- (1) We have analyzed the collision-induced relaxation of Eu atoms in the maximally stretched $m_s = 7/2$ level. We found that different hyperfine substates of the $m_s = 7/2$ manifold depopulate at the same rate, in agreement with the experimental observations. We confirmed that the bare (i.e., hyperfine-unmodified, state-independent) dipolar relaxation plays the dominant role in inducing the trap loss. We found that the collision energy dependence of cross sections for both elastic and inelastic scattering is modified by a manifold of shape resonances in a multiple partial-wave scattering regime. The elastic energy transfer is insensitive to the magnetic field, whereas the efficacy of Zeeman relaxation slightly increases as the magnetic field strength decreases.
- (2) By averaging the calculation results over magnetic fields and collision energies in the trap, we computed the rate constant for Zeeman relaxation of magnetically trapped Eu atoms. Our value of $8.6 \times 10^{-13} \text{ cm}^3/\text{s}$ is in reasonable agreement with the experimental value $(2.5 \pm 1.5) \times 10^{-13} \text{ cm}^3/\text{s}$. The possibility of direct evaporative cooling of Eu atoms was analyzed based on the calculations of the collision rate constants at cold and ultracold temperatures. The limiting temperatures of this technique for Eu were found to be similar to those observed previously for ^{52}Cr .
- (3) We have analyzed the role of the electronic spin-exchange interactions in determining transitions from the lower-energy Zeeman levels. Using an *ab initio* model [34], we demonstrated that the relaxation of the $m_s = 5/2$ state is very sensitive to the spin-exchange parameter J that determines the splitting between the spin states of the Eu_2 molecule. As a consequence of the spin anisotropy suppression for the submerged valence f shell in Eu atoms, the dipolar relaxation was shown to play the dominant role in trap loss of $m_s = 5/2$. We propose that cold collision experiments with multiple Zeeman states could be a promising way for obtaining accurate information on the electronic spin-exchange interaction in complex molecules such as Eu_2 .

ACKNOWLEDGMENTS

I am deeply indebted to Roman Krems and Alexei Buchachenko for stimulating this work, providing support, and critically reading the manuscript. Thanks are due to Alexei Buchachenko for providing the Eu-Eu interaction potentials prior to publication. I also thank Scott Habershon for useful comments. The allocation of computer time on the Western Canada Research Grid (WestGrid) and Research Cluster of the Roman Krems group (Feshbach) is gratefully acknowledged. The author acknowledges support from the British Academy, the Royal Society of Engineering, and the Royal Society. The research was also supported by NSERC of Canada and by the Russian Basic Research Fund (Project 08-03-00414).

-
- [1] R. deCarvalho, J. M. Doyle, B. Friedrich, T. Guillet, J. Kim, D. Patterson, and J. D. Weinstein, *Eur. Phys. J. D* **7**, 289 (1999).
 - [2] J. M. Doyle, B. Friedrich, J. Kim, and D. Patterson, *Phys. Rev. A* **52**, 2515R (1995).
 - [3] J. G. E. Harris, R. A. Michniak, S. V. Nguyen, N. Brahm, W. Ketterle, and J. M. Doyle, *Europhys. Lett.* **67**, 198 (2004).
 - [4] C. I. Hancox, S. C. Doret, M. T. Hummon, R. V. Krems, and J. M. Doyle, *Phys. Rev. Lett.* **94**, 013201 (2005).
 - [5] C. I. Hancox, S. C. Doret, M. T. Hummon, L. Luo, and J. M. Doyle, *Nature (London)* **431**, 281 (2004).
 - [6] J. D. Weinstein, R. deCarvalho, J. Kim, D. Patterson, B. Friedrich, and J. M. Doyle, *Phys. Rev. A* **57**, R3173 (1998).
 - [7] J. D. Weinstein, R. deCarvalho, C. I. Hancox, and J. M. Doyle, *Phys. Rev. A* **65**, 021604(R) (2002).
 - [8] R. deCarvalho, C. I. Hancox, and J. M. Doyle, *J. Opt. Soc. Am. B* **20**, 1131 (2003).
 - [9] S. V. Nguyen, R. deCarvalho, and J. M. Doyle, *Phys. Rev. A* **75**, 062706 (2007).
 - [10] J. G. E. Harris, S. V. Nguyen, S. C. Doret, W. Ketterle, and J. M. Doyle, *Phys. Rev. Lett.* **99**, 223201 (2007).
 - [11] S. V. Nguyen, J. S. Helton, K. Maussang, W. Ketterle, and J. M. Doyle, *Phys. Rev. A* **71**, 025602 (2005).
 - [12] C. I. Hancox, M. T. Hummon, S. V. Nguyen, and J. M. Doyle, *Phys. Rev. A* **71**, 031402(R) (2005).
 - [13] J. Kim, B. Friedrich, D. P. Katz, D. Patterson, J. D. Weinstein, R. DeCarvalho, and J. M. Doyle, *Phys. Rev. Lett.* **78**, 3665 (1997).
 - [14] R. V. Krems, G. C. Groenenboom, and A. Dalgarno, *J. Phys. Chem. A* **108**, 8941 (2004).
 - [15] R. V. Krems, J. Klos, M. F. Rode, M. M. Szczyński, G. Chałasiński, and A. Dalgarno, *Phys. Rev. Lett.* **94**, 013202 (2005).
 - [16] A. A. Buchachenko, M. M. Szczyński, and G. Chałasiński, *J. Chem. Phys.* **124**, 114301 (2006).
 - [17] A. A. Buchachenko, G. Chałasiński, M. M. Szczyński, and R. V. Krems, *Phys. Rev. A* **74**, 022705 (2006).
 - [18] Z. Pavlović, B. O. Roos, R. Côté, and H. R. Sadeghpour, *Phys. Rev. A* **69**, 030701(R) (2004).
 - [19] Z. Pavlović, R. V. Krems, R. Côté, and H. R. Sadeghpour, *Phys. Rev. A* **71**, 061402(R) (2005).
 - [20] A. Griesmaier, J. Werner, S. Hensler, J. Stuhler, and T. Pfau, *Phys. Rev. Lett.* **94**, 160401 (2005).
 - [21] J. Werner, A. Griesmaier, S. Hensler, J. Stuhler, T. Pfau, A. Simoni, and E. Tiesinga, *Phys. Rev. Lett.* **94**, 183201 (2005).
 - [22] J. Kim, Ph.D. thesis, Harvard University, 1997.
 - [23] L. Cai, B. Friedrich, and J. M. Doyle, *Phys. Rev. A* **61**, 033412 (2000).
 - [24] R. V. Krems, *Int. Rev. Phys. Chem.* **24**, 99 (2005).
 - [25] R. V. Krems and A. Dalgarno, *J. Chem. Phys.* **120**, 2296 (2004).
 - [26] R. V. Krems and A. Dalgarno, in *Fundamental World of Quantum Chemistry*, edited by E. J. Brändas and E. S. Kryachko (Kluwer, Amsterdam, 2004), Vol. 3, p. 273.
 - [27] R. V. Krems and A. Dalgarno, *Phys. Rev. A* **68**, 013406 (2003).

- [28] Z. Li and R. V. Krems, *Phys. Rev. A* **75**, 032709 (2007).
- [29] C. Cohen-Tannoudji, B. Diu, and F. Laloë, *Quantum Mechanics* (Wiley, New York, 2006), Vol. 2.
- [30] G. J. Zaal, W. Hogervorst, E. R. Eliel, K. A. H. van Leeuwen, and J. Blok, *Z. Phys. A* **290**, 339 (1979).
- [31] K. Takayanagi, *Adv. At. Mol. Opt. Phys.* **1**, 149 (1965).
- [32] T. V. Tscherbul, Yu. V. Suleimanov, V. Aquilanti, and R. V. Krems, *New J. Phys.* **11**, 055021 (2009).
- [33] D. E. Manolopoulos, *J. Chem. Phys.* **85**, 6425 (1986).
- [34] A. A. Buchachenko, G. Chałasiński, and M. M. Szczyński, *J. Chem. Phys.* **131**, 241102 (2009).
- [35] W. Heisenberg, *Z. Phys.* **49**, 619 (1928).
- [36] C. Herring, in *Magnetism*, edited by G. T. Rado and H. Suhl (Academic, New York, 1966), Vol. IIB.
- [37] A. A. Buchachenko, G. Chałasiński, and M. M. Szczyński, *Eur. Phys. J. D* **45**, 147 (2007).
- [38] E. P. Wigner, *Phys. Rev.* **73**, 1002 (1948).
- [39] R. V. Krems and A. Dalgarno, *Phys. Rev. A* **67**, 050704(R) (2003).
- [40] A. Kant and S. S. Lin, *Monatsh. Chem.* **103**, 757 (1972).
- [41] P. A. Montano, *J. Phys. C* **15**, 565 (1982).
- [42] P. L. Goodfriend, *Spectrochim. Acta* **40**, 283 (1984).
- [43] J. R. Lombardi and B. Davis, *Chem. Rev.* **102**, 2431 (2002).
- [44] M. Dolg, H. Stoll, and H. Preuss, *J. Mol. Struct., Theochem* **277**, 239 (1992).
- [45] X. Cao and M. Dolg, *Theor. Chem. Acc.* **108**, 143 (2002).